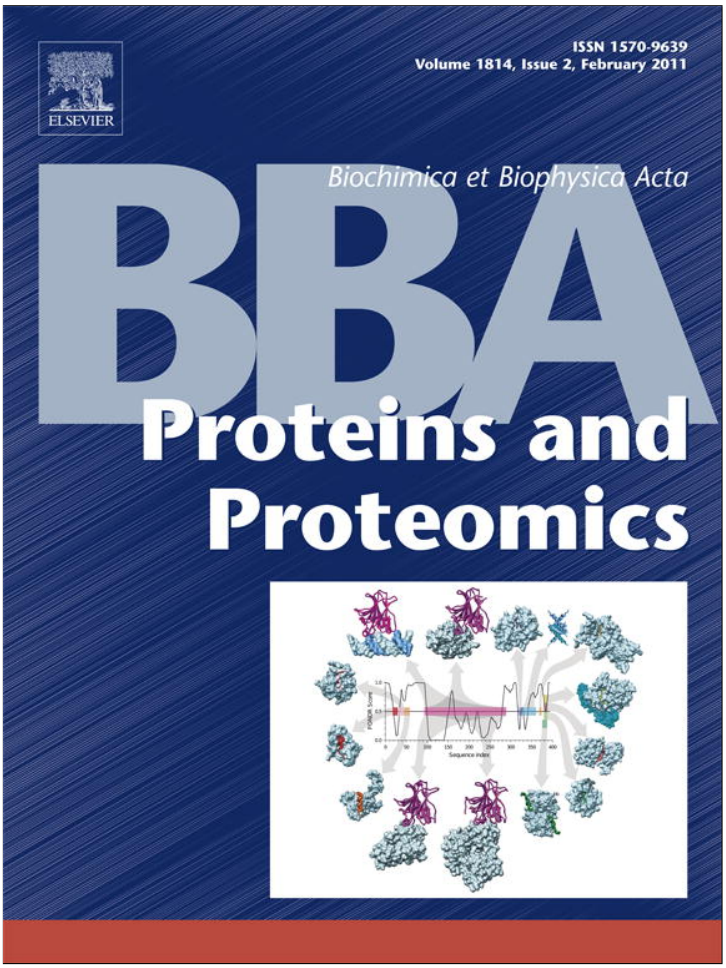

(This is a sample cover image for this issue. The actual cover is not yet available at this time.)

Biochimica et Biophysica Acta 1824 (2012) 334–338

Contents lists available at SciVerse ScienceDirect

Biochimica et Biophysica Acta

journal homepage: www.elsevier.com/locate/bbapap

Binding of the plant hormone kinetin in the active site of Mistletoe Lectin I from *Viscum album*

Piotr H. Małecki [a], Wojciech Rypniewski [a], Maciej Szymański [a], Jan Barciszewski [a], Arne Meyer [b,*]

[a] Institute of Bioorganic Chemistry, Polish Academy of Sciences, Noskowskiego 12/14, 61-704 Poznan, Poland
[b] Institute of Biochemistry and Molecular Biology, Laboratory for Structural Biology of Infection and Inflammation, University of Hamburg, c/o DESY Build. 22a, Notkestr. 85, 22603 Hamburg, Germany

ARTICLE INFO

Article history:
Received 25 July 2011
Received in revised form 13 October 2011
Accepted 17 October 2011
Available online 28 October 2011

Keywords:
Microgravity
Ribosome inactivation
Cytokinin
Active site
Kinetin

PDB ID:
3O5W

ABSTRACT

The crystal structure of the ribosome inhibiting protein Mistletoe Lectin I (ML-I) derived from the European mistletoe, *Viscum album*, in complex with kinetin has been refined at 2.7 Å resolution. Suitably large crystals of ML-I were obtained applying the counter diffusion method using the Gel Tube R Crystallization Kit (GT-R) on board the Russian Service Module on the international space station ISS within the GCF mission No. 6, arranged by the Japanese aerospace exploration agency (JAXA). Hexagonal bi-pyramidal crystals were grown during three months under microgravity. Before data collection the crystals were soaked in a saturated solution of kinetin and diffraction data to 2.7 Å were collected using synchrotron radiation and cryogenic techniques. The atomic model was refined and revealed a single kinetin molecule in the ribosome inactivation site of ML-I. The complex demonstrates the feasibility of mistletoe to bind plant hormones out of the host regulation system as part of a self protection mechanism.

1. Introduction

Cytokinins (CKs, plant hormones) were discovered during the 1950s as substances able to induce the division of plant cells. Natural CKs are N6-substituted adenine derivatives [1]. The first CK discovered was 6-furfuryladenine (kinetin) — a degradation product of DNA which promotes cell division in plants [2]. Since then, a substantial number of biochemical, physiological and genetic studies have focused on elucidating the diverse roles of CKs in plant growth and development, their levels in plants due to expression of bacterial genes, recovery of mutant plants with a higher CK content, and characterization of loss-of-function mutants of the CK receptor. They are also involved in other essential processes such as sink/source, vascular development, chloroplast differentiation, apical dominance and senescence [3]. It appears that those effects are a result of interactions with other plant hormones and environmental signals. Although the effects of cytokinins in plants are well known, the mechanism of their perception is still not understood. In addition to that, kinetin and other molecules with N6-substituted adenine show interesting properties which make them useful in molecular medicine [4,5].

Plant lectins are a heterologous group of proteins classified together on the basis of their ability to bind in a reversible way to well defined simple sugars and/or complex carbohydrates [6]. There is a common view that plant lectins are directed against foreign glycans and, accordingly, they are destined to interact with other organisms, either in recognition or in defence-related phenomena. In addition to the lectin carbohydrate binding affinity a number of lectins have quaternary structure-based hydrophobic sites capable of accommodating various hydrophobic ligands e.g. N6-substituted adenine derivatives [7]. The binding of non-carbohydrate ligands to lectins demonstrates the bifunctional nature of these proteins.

They can be classified in two groups. There are seven families of proteins in the first group and the second group consists of ribosome inactivating proteins (RIPs). The later group are heterodimeric plant proteins with a carbohydrate binding B chain and an enzymatic A-chain which acts on ribosomes to inhibit protein synthesis. RIPs are a group of cytosolic N-glycosidases that specifically cleave the N–C glycosidic bond. Three types of them can be distinguished: I — simple polypeptide chain, II — chain A functionally equivalent to type I with a B-chain with a lectin function and III — single chain containing an extended carboxy-terminal domain of unknown function [8,9].

ML-I is a heterodimeric protein consisting of a carbohydrate-binding chain B (lectin) joined by a single disulphide bond to a catalytic subunit A: a RIP type II that cleaves the *N*-glycosidic bond of a specific adenine

* Corresponding author at: Institute of Biochemistry, University of Lübeck, Laboratory for Structural Biology of Infection and Inflammation, c/o DESY Build. 22a, Notkestr. 85, 22603 Hamburg, Germany. Tel.: +49 40 8998 4746; fax: +49 40 8998 4747.
E-mail address: meyer@biochem.uni-luebeck.de (A. Meyer).

1570-9639/$ – see front matter © 2011 Elsevier B.V. All rights reserved.
doi:10.1016/j.bbapap.2011.10.013

residue from 28S rRNA. The bipartite molecular structure of ML-I allows it to bind to the mammalian cell surface, to enter via endocytic uptake and to deliver the catalytically active polypeptide into the cytoplasm where it inhibits protein synthesis analogously to the best known example of type II lectins — ricin [10]. To investigate substrate binding properties of ricin the X-ray structures have been solved for complexes with the adenosine analogue, formycin monophoshate (FMP) and the dinucleoside monophosphate ApG [11]. Adenosine binds in the ricin chain A active site. It stacks with the aromatic side chains of two tyrosine residues. Specific hydrogen bonds are formed between the Val 77 carbonyl O-atom of the toxin and the N1 and N6 group of the adenine ring, mimicking a Watson–Crick base pair. A catalytic mechanism has been proposed by Monzingo and Robertus [11]. In the case of ML-I the target adenosine is stacked with the aromatic side chains of Tyr 76 and Tyr 115 of chain A. Specific hydrogen bonds are formed to the adenine ring analogue to Watson–Crick base pairing. Cleavage of the *N*-glycosidic bond between adenine N9 and C1′ of the ribose is facilitated by protonation at N3 by water and thereby activates the solvent as it develops a hydroxide character. Ion pairing of Glu 165 stabilizes the cationic development of the oxycarbonium ion on the ribose, whereas the activated water molecule attacks the oxycarbonium releasing the adenine leaving group.

2. Material and methods

2.1. Protein purification

Native plant material consisting of leaves and stems has been used for isolating the protein. The crude material of the European mistletoe (*Viscum album*) growing on apple trees (*Malus domestica*) was used, collected in the period February to March. Purification of ML-I for crystallization was carried out according to the previously described procedures [12]. After removing fruits, leaves as well as small branches were flash-frozen, ground into powder, dissolved in water and centrifuged. The supernatant was loaded on an affinity column of lactose immobilized with divinyl sulphone [13]. Afterwards lectins were separated using aminophenyl-boronic-acid-affinity chromatography [14]. For crystallization ML-I was dialyzed against 0.2 M glycine–HCl buffer at pH 2.5, as described in detail in Krauspenhaar et al. [15].

2.2. Crystallization

High quality crystals of ML-I were obtained using the counter diffusion method in Granada Crystallization Boxes (GCB, Hampton Research) applying the Gel-Tube R (GT-R) method [16] instead of the original gel-acupuncture method having the following crystallization parameters and configuration specifications: protein concentration 5 mg/ml in 0.2 M glycine/HCl, pH 2.5. Initial concentration of the precipitant solution was 1.0 M ammonium sulphate in 0.2 M glycine/HCl, pH 2.5. Capillary length was 75 mm with an inner diameter of 0.5 mm. Mini Gel-Tube length was 15 mm after attachment of the lower end of the capillary the remaining gel length was 10 mm. Six capillaries were used in a single GCB 2. Depth of precipitant solution was 66 mm. Protein solution length was 55 mm. The experiment was performed at 20 °C. Typical hexagonal bi-pyramidal crystals of ML-I have been obtained during the 109 days under microgravity on board the Russian Service Module on the ISS during the JAXA GCF flight No. 6. The crystals were retrieved from the capillaries into a soaking solution containing 1.0 M ammonium sulphate in 0.2 M glycine/HCl, pH 2.5 saturated with kinetin, and were soaked for 2 h.

2.3. Data collection and processing

X-ray diffraction data were collected up to 2.7 Å resolution using a 165 mm MAR CCD detector at the consortium beam line X13 (HASYLAB/DESY), using crystals frozen and stabilized at 100 K. Prior to flash freezing the crystals were soaked in a solution containing 20% v/v glycerol in the reservoir solution saturated with kinetin in order to avoid ice formation. Data processing and scaling were carried out using DENZO and SCALEPACK [17]. MLI crystals belong to space group $P6_522$ with a single molecule in the asymmetric unit. Unit cell parameters were $a = b = 107.6$ Å and $c = 310.6$ Å. The packing parameter V_M was calculated to be 4.4 Å/Da [18], which corresponded to a solvent content of 75%. Data collection and scaling statistics are summarized in Table 1.

2.4. Structure determination and refinement

The isomorphous X-ray structure of the ML-I-AMP complex (PDB ID: 1M2T) [15] was used, after removing the solvent and ligand atoms, for the initial model building and refinement. Further refinement was carried out applying the program Refmac 5 [19,20]. A subset of 5% of the reflections was excluded from refinement and used only for the R_{free} statistics [21]. Manual rebuilding of the model and electron intensity interpretation was done using the graphics program Coot [22]. Ligand molecules were identified using maps calculated with the coefficients F_o–F_c. The electron density was visualized using $2F_o$–F_c maps. ML-I is known to have four potential NAG *N*-glycosylation sites, characterized by sequence motifs Asn-X-Ser/Thr [10]. The sites are at Asn 112 in subunit A and Asn 308, Asn 343 and Asn 383 in subunit B. In the course of the refinement, F_o–F_c maps showed carbohydrate densities at all the four glycosylation sites. However, only one NAG residue could be identified at Asn 112, two at Asn 308 and Asn 343, each, and three NAG residues at Asn 383. These saccharides were included in the model and subsequently refined. Water molecules were identified using the solvent building function of Coot. The structure of the complex was refined to an R value of 0.17 and R_{free} of 0.23 for all data between 20.0 and 2.8 Å resolution. The refinement statistics are summarized in Table 1.

Table 1
Data collection and refinement parameters.

X-ray source	DESY, Hamburg, beam l ine X13
Temperature (K)	100
Resolution range (Å)	20.0–2.70
Wavelength (Å)	0.820
Space group	$P6_522$
Cell parameters (Å)	$a = b = 107.6$, $c = 310.6$
No. observations	980,547
No. unique reflections	28,527
R_{merge}[a]	0.137
Completeness (%)	99.1
Average I/σ(I)	13
I/σ(I) in high-resolution bin	1.8
Mosaicity (°)	0.3
Data multiplicity	9.0
Final R/R_{free}	0.174/0.226
No. protein atoms	3922
No. solvent molecules	310
Other atoms	181
Average B factors (Å^2)	47.4
Protein	46
Solvent	46
Ligand	78
R.m.s.d. from ideal bond length (Å)	0.02
R.m.s.d. from ideal bond angles (°)	2.05
Ramachandran plot, % residues in regions (PROCHECK)	
Most favoured	87.4
Additionally allowed	12
Generously allowed	0.6
Disallowed	0

[a] $R_{merge} = \sum_{hkl} \sum_i |I_i\ (hkl) - <I(hkl)>| / \sum_{hkl} \sum_i I_i\ (hkl)$, where $I_i\ (hkl)$ and $<I(hkl)>$ are the observed individual and mean intensities of a reflection with the indices *hkl*, respectively, $\sum_i$ is the sum over *i* measurements of a reflection with the indices *hkl*, and $\sum_{hkl}$ is the sum over all reflections.

3. Results

3.1. The overall crystal structure and model quality

The refined X-ray model consisted of a single ML-I molecule, one kinetin molecule, one sulphate ion, 8 glycerol molecules and 310 ordered water molecules. The protein model consisted of 510 amino acid residues in two chains (chain A, 1–248 and chain B, 249–510) and 8 glycan residues at four glycosylation sites: at Asn 112, Asn 308, Asn 343 and Asn 383. The overall structure is shown in Fig. 1. Chain A is folded into three domains. Domain I (residues 1–109) is rich in β-structures while domain II (residues 110–198) consists mainly of α-helices. Domain III of chain A consists of residues 199–249 and some parts interact with second chain. Chain B consists of two globular domains, presumably a result of gene duplication, similar to those reported for ricin [23]. However, there is no detectable sequence similarity between the topologically similar domains and their galactose-binding sites also differ [24]. The program PROCHECK was used to validate the final model [25]. 95% of the residues were in the most favoured regions of the Ramachandran plot and the remaining residues were in the additionally allowed regions. Details of the data statistics and refinement are summarised in Table 1.

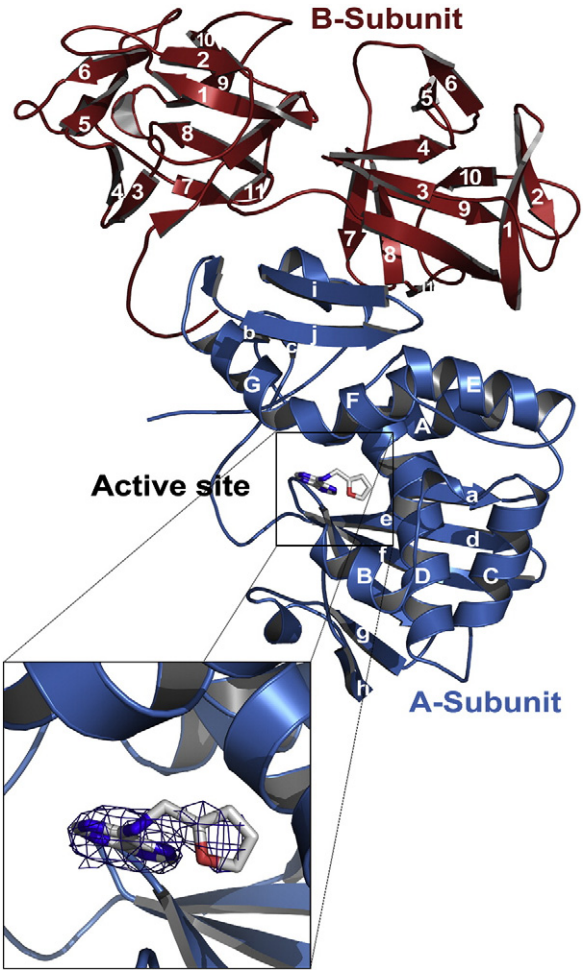

Fig. 1. Cartoon plot of ML-I with bound kinetin. The three domains of the A-chain are labelled I (a, A, b–h), II (B–F) and III (i, j, G) and coloured blue. The α-helices of the secondary structure are labelled with capital letters, β-sheets in lower case. The two domains of the B-chain are coloured red. Weighted $2F_o–F_c$ map, contoured at the 1 σ level, is shown for kinetin. This and the other figures were prepared with the program PyMOL [33]. (For interpretation of the references to colour in this figure legend, the reader is referred to the web version of this article.)

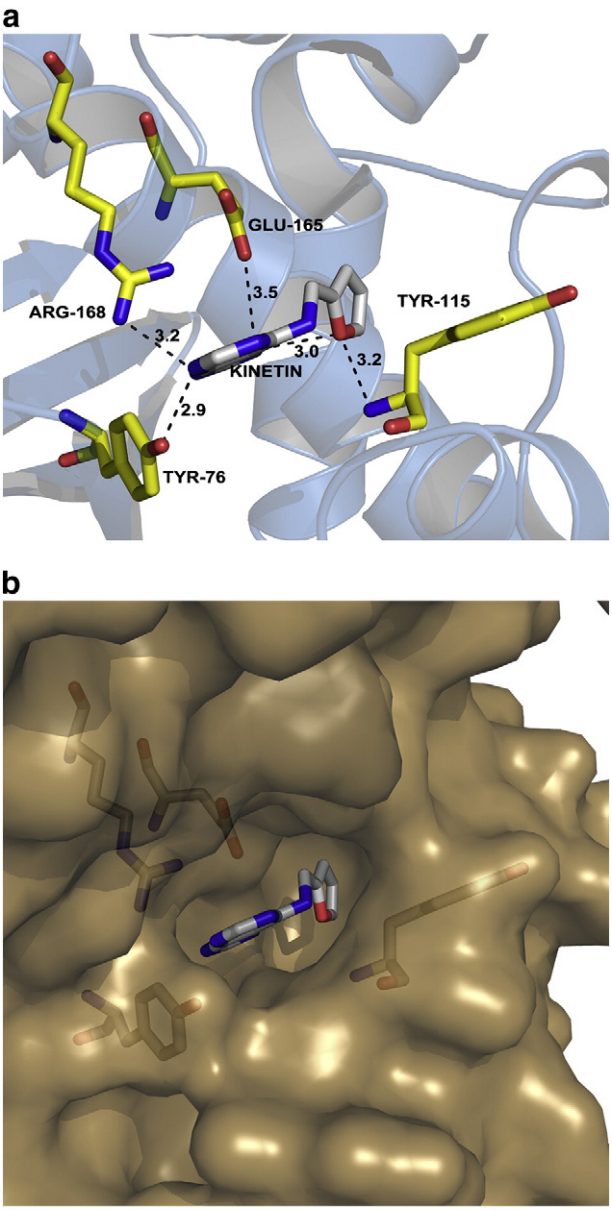

Fig. 2. (a) Details of the interaction between the kinetin and ML-I. Hydrogen bonds with the protein's active site residues are indicated as dashed lines. Acceptor–donor distance are in Å. (b) Surface representation showing the ligand binding cavity.

3.2. Kinetin binding

One kinetin molecule has been identified, based on the $F_o–F_c$ map, in the active site of ML-I (Fig. 2a). Kinetin is bound near the surface of the protein, so the purine group is partially accessible to the environmental solvent (Fig. 2b). The distance and character of interactions of the ligand with the protein indicates a number of hydrogen bonds between the kinetin and all the conserved residues that have been proposed to be important for catalytic activity: Tyr 76, Tyr 115, Glu 165 and Arg 168 [26]. The hydroxyl oxygen of Tyr 76 is at a H-bonding distance from the N3 atom of kinetin (2.9 Å). Arg 168 is stabilized by stacking with Trp 199 and H-bonds with O Asn 74 and the carboxyl O of Glu 165, while one of its Nη atoms interacts with kinetin's N9 (3.2 Å). Glu 165 is in a possible position to establish a hydrogen bond with N7 of the ligand's adenine moiety but the distance of 3.5 Å indicates a weak interaction. The furfuryl group is stabilised by a single hydrogen bond between its O atom and the N atom of

Tyr 115 (3.2 Å). The conformation of the kinetin molecule is stabilised by an intramolecular H-bond between N7 and O15 (3.0 Å).

Examination of the hydrogen bond network around the kinetin indicates the 7H-amino tautomeric form of the bound molecule: N7 acts as a donor of H-bonds, therefore it must be protonated, while the N9 atom is an acceptor and is deprotonated [27].

The orientation of the adenine residue of kinetin is quite different from the position of the adenine ring observed in the binding study of ATP to ML-I [15] (Fig. 3). The plane of the adenine moiety in the present structure is approximately orthogonal to the binding plane of unsubstituted adenine. This reorientation is coupled with shifting of the Tyr 76 side chain. Also the N6 atom of kinetin points in a different direction and consequently the furfuryl substituent occupies the place of Tyr 115 side chain, which is now turned by approx. 125° towards the solvent space, out of its position in the complex with the unsubstituted adenine. The movement of Tyr 115 interrupts its stacking interaction with Arg 125, whose guanidinium group is now flipped and engaged, via two H-bonds, with a sulphate anion. The sulphate, which is found in all ML-I structures that do not have adenine bound, is also coordinated by His 124 and Asp 126 (Fig. 3). In the only other, to our knowledge, known structure of kinetin interacting with a protein, kinetin binds at the active site of a chitinase from *Saccharomyces cerevisiae* [28] and inhibits strongly. The contacts there include both hydrogen bonds and aromatic stacking of the adenine ring with the protein's tryptophane side chain. In this respect the mode of binding appears quite different from the present case, where only H-bonding contacts are observed.

4. Discussion

Although kinetin binds in the active site of ML-I, its orientation is different from that observed for unmodified adenine in the ATP binding study [15]. In a previous study, formycin monophosphate, a nucleotide analogue, was found to bind to ricin in a similar manner as adenine binds to ML-I [11]. Several other ligands have been found to bind to ricin with their aromatic ring wedged between two Tyr residues equivalent to Tyr 115 and Tyr 76 of ML-I [29,30]. Therefore, it seems reasonable to propose that the different binding mode of kinetin in the present study is related to the presence of the furfuryl substituent at N6. In order for it to bind the adenine ring in similar orientation as in the other compounds, the N6-substituent would have to penetrate the interior of the protein, which would entail substantial rearrangements of residues. In the present structure it binds without causing major structural changes to the ML-I, compared to the protein's unliganded state. One possible exception is Tyr 115 which in the presence of kinetin is in an 'open' conformation, making way for the ligand's furfuryl ring (Fig. 3). However, in one other structure Tyr 115 has been observed to take up the 'open' position (thus increasing the volume of the binding site cavity) even when there is no ligand in the active site [31], thus the tyrosine seems to be able to take up easily one of the two positions.

It is interesting to observe a ligand binding in an enzyme's active site in a way that is quite different from the binding of the substrate. A design of inhibitors usually relies on the knowledge of substrate binding specificity, which has obvious advantages but carries the danger that a designed ligand will undergo enzymatic degradation. The different orientation of bound kinetin and the alternative engagement of the enzyme's catalytic residues make it unlikely that the enzyme can be active against such a ligand. This appears consistent with our attempts to co-crystallise ML-I with kinetin riboside, which were unsuccessful (unpublished). X-ray analysis revealed an unoccupied active site, probably because accommodating the additional ribose ring would result in steric clashes in the active site. If, on the other hand, the riboside was processed by the enzyme, one would expect to find kinetin in the active site.

The binding of kinetin to ML-I is quite different from the binding of a related cytokinin, zeatin, whose binding site was found to be in a central

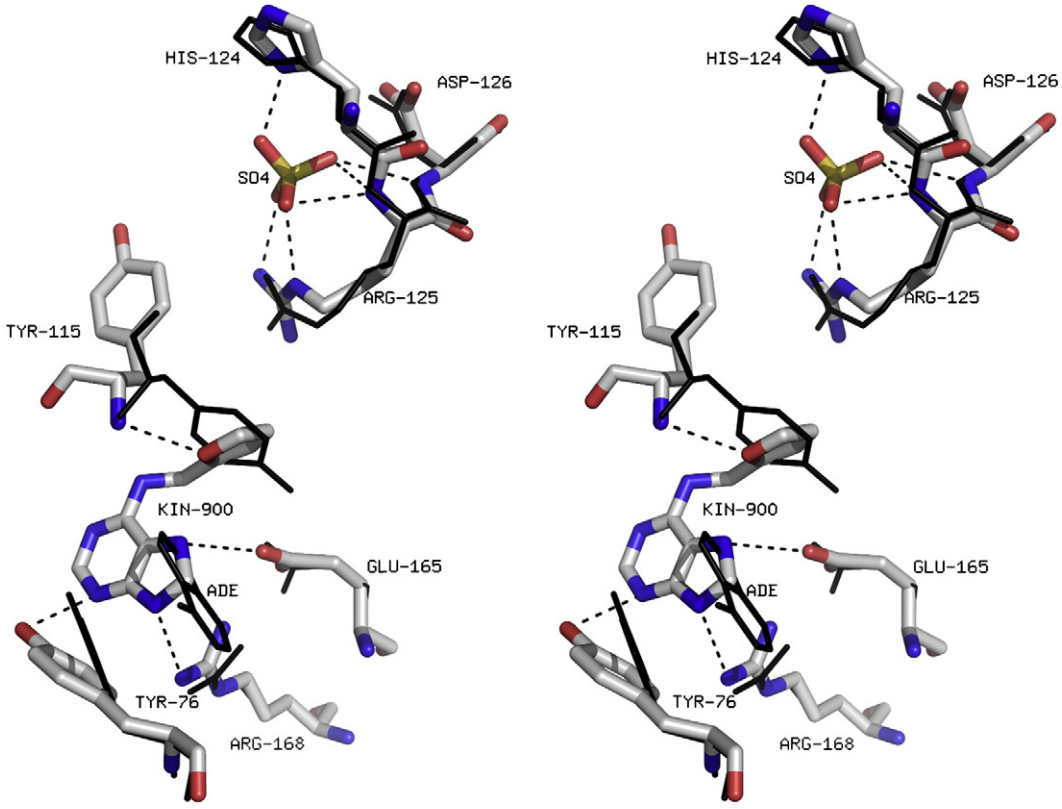

Fig. 3. Stereo figure showing a comparison of ML-I in complex with kinetin (coloured sticks) towards the ML-I/adenine complex (black bonds). Different binding modes of the ligands are accompanied by significant rearrangements of the active site residues, especially Tyr 115. The bound sulphate ion is present only in the ML-I/kinetin complex.

cavity between the two ML-I subunits [32], and from the binding of another plant hormone, phloretamide which also binds in the centre of the protein [31].

5. Conclusion

The binding of kinetin in ML-I's active site is potentially related to the protein's well known function as a ribosome inactivating agent, but the significance of the interaction with kinetin is still unclear. It is clear, however, that the complex interplay between the host and the parasite has to include mechanisms of dealing with each other's hormonal signalling, as their life cycles are different. Powerful substances, such as cytokinins, have to be controlled. It is possible that the binding of kinetin to ML-I is fortuitous, but this would be contrary to the nature of hormones, which by definition are present in very low concentrations and in order to be effective they have to be accurately targeted. A potential ancillary function of ML-I is to sequester stray potentially disruptive cytokinins diffusing in from the host organism.

Acknowledgements

The work was supported by grants from the Deutsche Luft- und Raumfahrtagentur, DLR under Project number: 50WB0615and via project IND 10/107, by the Ministry of Science and Higher Education (Poland, grant PBZ-MNiSW-07/I/2007/11). The project was also co-funded by European Union within European Regional Development Fund.

References

[1] R.M. Amasino, Kinetin arrives. The 50th anniversary of a new plant hormone, Plant Physiol. 138 (2005) 1177–1184.
[2] C.O. Miller, F. Skoog, M.H. von Saltza, F.M. Strong, Structure and synthesis of kinetin, J. Am. Chem. Soc. 77 (1955) 1392.
[3] D.W. Mok, M.C. Mok, Cytokinin metabolism and action, Annu. Rev. Plant Physiol. Plant Mol. Biol. 52 (2001) 89–118.
[4] S.I.S. Rattan, N6-furfuryladenine (kinetin) as a potential anti-aging molecule, J. Anti Aging Med. 5 (2002) 113–116.
[5] J. Barciszewski, G. Siboska, S.I.S. Rattan, B.F.C. Clark, Occurrence, biosynthesis and properties of kinetin (N6-furfuryladenine), Plant Growth Regul. 32 (2000) 106–115.
[6] E.J. Van Damme, A. Barre, P. Rouge, W.J. Peumans, Cytoplasmic/nuclear plant lectins: a new story, Trends Plant Sci. 9 (2004) 484–489.
[7] E.J. Zaluzec, M.M. Zaluzec, K.W. Olsen, S.F. Pavkovic, Crystallization and preliminary X-ray analysis of peanut agglutinin-N^6-benzylaminopurine complex, J. Mol. Biol. 219 (1991) 151–153.
[8] S.W. Park, R. Vepachedu, N. Sharma, J.M. Vivanco, Ribosome-inactivating proteins in plant biology, Planta 219 (2004) 1093–1096.
[9] M. Ambrosi, N.R. Cameron, B.G. Davis, Lectins: tools for the molecular understanding of the glycocode, Org. Biomol. Chem. 3 (2005) 1593–1608.
[10] J.M. Lord, L.M. Roberts, J.D. Robertus, Ricin: structure, mode of action, and some current applications, FASEB J. 8 (1994) 201–208.
[11] A.F. Monzingo, J.D. Robertus, The three-dimensional structure of ricin at 2.8 A, J. Mol. Biol. 227 (1992) 1136–1145.
[12] W. Voelter, R. Wacker, S. Stoeva, R. Tsitsilonis, C. Betzel, Mistletoe lectins, structure and function, Front. Nat. Prod. Chem. 1 (2005) 149–162.
[13] S. Crider-Pirkle, P. Billingsley, C. Faust, C.D.M. Hardy, V. Lee, H. Weitlauf, Cubilin, a binding partner for galectin-3 in the murine utero-placental complex, J. Biol. Chem. 277 (2002) 15904–15912.
[14] Y.C. Li, U. Pfuller, E.L. Larsson, H. Jungvid, I.Y. Galaev, B. Mattiasson, Separation of mistletoe lectins based on the degree of glycosylation using boronate affinity chromatography, J. Chromatogr. 925 (2001) 115–121.
[15] R. Krauspenhaar, W. Rypniewski, N. Kalkura, K. Moore, L. DeLucas, St. Stoeva, A. Mikhailov, W. Voelter, Ch. Betzel, Crystallisation under microgravity of mistletoe lectin I from *Viscum album* with adenine monophosphate and the crystal structure at 1.9 A resolution, Acta Crystallogr., Sect. D: Biol. Crystallogr. 58 (2002) 1704–1707.
[16] H. Tanaka, K. Inaka, S. Sugiyama, S. Takahashi, S. Sano, M. Sato, S. Yoshitomi, A simplified counter diffusion method combined with a 1D simulation program for optimizing crystallization conditions, J. Synchrotron Radiat. 11 (2004) 45–48.
[17] Z. Otwinowski, W. Minor, Processing of X-ray diffraction data collected in oscillation mode, Methods Enzymol. 276 (1997) 307–326.
[18] B.W. Matthews, Solvent content of protein crystals, J. Mol. Biol. 33 (2) (1968) 491–497.
[19] Collaborative Computational Project, Number 4, Acta Crystallogr., Sect. D: Biol. Crystallogr. 50 (1994) 760.
[20] A.A. Vagin, R.A. Steiner, A.A. Lebedev, L. Potterton, S. McNicholas, F. Long, G.N. Murshudov, Refmac5 dictionary: organization of prior chemical knowledge and guidelines for its use, Acta Crystallogr., Sect. D: Biol. Crystallogr. 60 (2004) 2184–2195.
[21] A.V. Lyashenko, N.E. Zhukhlistova, A.G. Gabdoulkhakov, Y.N. Zhukova, W. Voelter, V.N. Zaitsev, I. Bento, E.V. Stepanova, G.S. Kachalova, O.V. Koroleva, E.A. Cherkashyn, V.I. Tishkov, V.S. Lamzin, K. Schirwitz, E.Y. Morqunova, C. Betzel, P.F. Lindley, A.M. Mikhailov, Crystal structure of laccase from Cerrena maxima at 1.9 A resolution, Acta Crystallogr. Sect. F Struct. Biol. Cryst. Commun. 62 (2006) 954–957.
[22] P. Emsley, K. Cowtan, Coot: model-building tools for molecular graphics, Acta Crystallogr., Sect. D: Biol. Crystallogr. 60 (2004) 2126–2132.
[23] W. Montfort, J.E. Villafranca, A.F. Monzingo, S.R. Ernst, B. Katzin, E. Rutenber, N.H. Xoung, R. Hamlin, J.D. Robertus, J. Biol. Chem. 262 (1987) 5398–5403.
[24] R. Mikeska, R. Wacker, R. Arni, T.P. Singh, A. Mikhailov, A. Gabdoulkhakov, W. Voelter, C. Betzel, Structures of Mistletoe Lectin I in complex with galactose and lactose reveals distinct sugar-binding properties, Acta Crystallogr., Sect. F Struct. Biol. Cryst. Commun. 61 (2005) 17–25.
[25] R.A. Laskowski, M.W. MacArthur, D. Moss, J.M. Thornton, PROCHECK — a program to check the stereochemical quality of protein structures, J. Appl. Crystallogr. 26 (1993) 283–291.
[26] G. Funatsu, M.R. Islam, Y. Minami, K. Sung-Sil, M. Kimura, Conserved amino acid residues in ribosome-inactivating proteins from plants, Biochimica 73 (1991) 1157–1161.
[27] G. Slosarek, M. Kozak, J. Gierszewski, A. Pietraszko, Structure of N^6-furfurylaminopurine (kinetin) dihydrogenphosphate, Acta Crystallogr., Sect. B: Struct. Sci. 62 (2006) 102–108.
[28] R. Hurtado-Guerrero, D.M. van Aalten, Structure of *Saccharomyces cerevisiae* chitinase 1 and screening-based discovery of potent inhibitors, Chem. Biol. 14 (2007) 589–599.
[29] D.J. Miller, K. Ravikumar, H. Shen, J.K. Suh, S.M. Kerwin, J.D. Robertus, J. Med. Chem. 45 (2002) 90–98.
[30] Y. Bai, A.F. Monzingo, J.D. Robertus, The X-ray structure of ricin A chain with a novel inhibitor, Arch. Biochem. Biophys. 483 (1) (2009) 23–28.
[31] A. Meyer, W. Rypniewski, L. Celewicz, V.A. Erdmann, W. Voelter, T.P. Singh, N. Genov, J. Barciszewski, Ch. Betzel, The mistletoe lectin I-phloretamide structure reveals a new function of plant lectins, Biochem. Biophys. Res. Commun. 364 (2007) 195–200.
[32] A. Meyer, W. Rypniewski, M. Szymanski, W. Voelter, J. Barciszewski, Ch. Betzel, Structure of mistletoe lectin I from *Viscum album* in complex with the phytohormone zeatin, Biochim. Biophys. Acta 1784 (2008) 1590–1595.
[33] W.L. DeLano, The PyMOL Molecular Graphics System, DeLano Scientific, San Carlos, CA, USA, 2002http://www.pymol.org.